Supporting Information: On the Ion Mobilities, Transference Numbers and Inverse Haven Ratios of Polymeric Ionic Liquids

Zidan Zhang,[†] Bill K Wheatle,[†] Jakub Krajniak,[‡] Jordan R Keith,[†] and Venkat Ganesan[*,†]

†*Department of Chemical Engineering, University of Texas at Austin, Austin, Texas 78712, United States*

‡*Independent researcher, os. Kosmonautow 13/56, 61-631 Poznan, Poland*

E-mail: venkat@che.utexas.edu

S1 Nernst-Einstein Conductivities for Electrolytes Containing Polycations and Free Anions

The conductivity σ of an electrolyte in a molecular simulation of volume V with n_a anions and n_c cations can be calculated by finding the slope of the linear, long-time portion of the following Einstein-type relationship:

$$\sigma = \lim_{t\to\infty} \frac{e^2}{6Vk_BT}\frac{\mathrm{d}}{\mathrm{d}t}\sum_{i,j=1}^{n_c+n_a} z_i z_j \langle [\Delta\mathbf{r}_i(t)]\cdot[\Delta\mathbf{r}_j(t)]\rangle \tag{S1}$$

Here e, k_B, T, z_i, $\Delta\mathbf{r}_i(t)$ are the proton charge, Boltzmann constant, temperature, scaled charge of ion i, and displacement of ion i. $\langle\cdots\rangle$ represents the ensemble average of the quantity represented by $\cdots$. The correlation in Eq. S1 can be broken into self and distinct parts:

$$\sum_{i,j=1}^{n_c+n_a} z_i z_j \langle [\Delta\mathbf{r}_i(t)]\cdot[\Delta\mathbf{r}_j(t)]\rangle = \sum_{i}^{n_c+n_a} z_i^2 \langle [\Delta\mathbf{r}_i(t)]^2\rangle + \sum_{i\neq j}^{n_c+n_a} z_i z_j \langle [\Delta\mathbf{r}_i(t)]\cdot[\Delta\mathbf{r}_j(t)]\rangle \tag{S2}$$

Letting the scaled charges of all cations and anions be z_c and z_a, respectively, we recognize that term one in Eq. S2 is related to the ionic diffusivities:

$$\lim_{t\to\infty}\frac{\mathrm{d}}{\mathrm{d}t}\sum_{i}^{n_c+n_a} z_i^2\langle [\Delta\mathbf{r}_i(t)]^2\rangle = 6(z_c^2 n_c D_c + z_a^2 n_a D_a) \tag{S3}$$

Here D_c and D_a are the diffusitivities of the cation and the anion, respectively. The Nernst-Einstein conductivity σ_{NE} is the conductivity in which it is assumed that there are no correlations between distinct ions. In the case of a simple electrolyte, in which all ions are unbound to each other, this causes term two to equal 0 $\forall\ i \neq j$. Assuming a symmetric electrolyte in which $z_c = -z_a = z$, electroneutrality demands that $n_c = n_a$. These considerations

simplifies Eq. S1 to yield σ_{NE} for a simple, symmetric electrolyte:

$$\sigma_{NE} = \frac{(ze)^2 n_c}{k_B T}(D_c + D_a) \tag{S4}$$

Defining the salt concentration $\rho = (n_c + n_a)/V$:

$$\sigma_{NE} = \frac{(ze)^2 \rho}{2k_B T}(D_c + D_a) \tag{S5}$$

We now assume that the electrolyte consists of polycations and unbound anions. There are m_c polycation chains with N_c charged repeat units. Each repeat unit has scaled charge z_c, and each anion has scaled charge z_a. Again assuming $z_c = -z_a = z$, now $n_a = N_c m_c$ to maintain electroneutrality. The derivation of σ_{NE} can be taken from the perspective of (1) the whole polycation chain as the positive charge carrier ($n_c = m_c$, $z_{cat} = N_c z_c$) or (2) each individual cation as the positive charge carrier ($n_c = N_c m_c$, $z_{cat} = z_c$), where z_{cat} is now defined as the positive charge carrier scaled charge. We evaluate perspective (1) below first.

Again we split the correlation in Eq. S1 into its self and distinct terms. Again, the first term is related to the ionic diffusivities:

$$\lim_{t\to\infty} \frac{\mathrm{d}}{\mathrm{d}t} \sum_{i}^{n_c+n_a} z_i^2 \langle [\Delta \mathbf{r}_i(t)]^2 \rangle = 6(z_{cat}^2 n_c D_{cat} + z_a^2 n_a D_a) \tag{S6}$$

Here D_{cat} and D_a are the diffusivities of the polycation's center of mass and the anion, respectively. From perspective (1), the second term in Eq. S1 in which $i \neq j$ goes to 0 as it did for the simple electrolyte. Combining Eq. S6 with Eq. S1, defining the salt concentration as the molar concentration of charged molecules $\rho = (m_c + N_c m_c)/V$, substituting the perspective (1) definitions of n_c, n_a, z_{cat}, z_a, and rearranging terms yields the definition of

σ_{NE} for a symmetric electrolyte whose positive charge carrier is a polycation:

$$\sigma_{NE} = \frac{(ze)^2}{k_B T}\rho\left(\frac{N_c^2}{N_c+1}D_{cat} + \frac{N_c}{N_c+1}D_a\right) \tag{S7}$$

From perspective (2), not all $i \neq j$ terms in Eq. S2 go to 0. While the motion of most ions remain uncorrelated, the motion of all cations on a given chain k are perfectly correlated at long times. Double summing over monomers $i \neq j$ on each of the m_c chains in the electrolyte appropriately the distinct term in Eq. S2 simplifies:

$$\begin{aligned}\sum_{k=1}^{m_c}\sum_{i\neq j}^{N_c}\langle[\Delta\mathbf{r}_{ki}(t)]\cdot[\Delta\mathbf{r}_{kj}(t)]\rangle &= \sum_{k=1}^{m_c}\sum_{i\neq j}^{N_c}\langle[\Delta\mathbf{r}_{ki}(t)]^2\rangle \\ &= (N_c-1)\sum_{k=1}^{m_c}\sum_{i}^{N_c}\langle[\Delta\mathbf{r}_{ki}(t)]^2\rangle\end{aligned} \tag{S8}$$

In a way similar to what we did in Eq. S6, we recognize that the long-time slope of the final term of Eq. S8 is related the polycation monomer diffusion coefficient D_c:

$$\lim_{t\to\infty}\frac{\mathrm{d}}{\mathrm{d}t}(N_c-1)\sum_{k=1}^{m_c}\sum_{i}^{N_c}\langle[\Delta\mathbf{r}_{ki}(t)]^2\rangle = 6m_cN_c(N_c-1)D_c \tag{S9}$$

Here $D_c = D_{cat}$ in Eq. S6, as the motion of each polycationic center-of-mass is perfectly correlated with each of its monomers. The long-time slope of term 1 in Eq. S2 is again related the ionic diffusivities:

$$\lim_{t\to\infty}\frac{\mathrm{d}}{\mathrm{d}t}\sum_{i}^{n_c+n_a} z_i^2\langle[\Delta\mathbf{r}_i(t)]^2\rangle = 6z^2m_cN_c(D_c+D_a) \tag{S10}$$

Combining Eq. S8 and Eq. S10 with Eq. S1 and defining the salt concentration again as

$\rho = (m_c + N_c m_c)/V$ yields the same form as Eq. S7:

$$\sigma_{NE} = \frac{(ze)^2}{k_B T}\rho\left(\frac{N_c^2}{N_c+1}D_c + \frac{N_c}{N_c+1}D_a\right) \tag{S11}$$

As an aside we compare Eqs. S7 and S11 to Eq. S5. If the degree of polymerization $N_c = 1$, perspectives (1) and (2) become equivalent and yields a simple electrolyte. Such an assumption yields a concentration c in Eqs. S7 and S11 equivalent to that in Eq. S5. Finally, the ratios $N_c^2/(N_c+1)$ and $N_c/(N_c+1)$ become both equal to $1/2$. Thus, Eqs. S7 and S11 become equivalent to Eq. S5 in the limit of simple electrolytes.

S2 Simulation Details

S2.1 Equilibirum Simulation

In this work, we used atomistic molecular dynamics (MD) simulations to probe the transference numbers and inverse Haven ratios spanning the spectrum from ILs to polyILs. Specifically, we considered the system of 1-butyl-3-methylimidazolium hexafluorophosphate ILs and quantified the influence of the degree of polymerization N on the transference number and inverse Haven ratio.

The setup of the systems can be found in Table S1. The polyIL chains and counterions PF_6^- were packed randomly into the initial simulation box with a box length of 12 nm, and the system contained a total of 1600 ion pairs. A multi-step equilibration procedure was used to prepare the equilibrated configuration for the production run.

1. Energy minimization via steepest-decent
2. 0.1 ns NVT simulation at 800 K
3. 0.1 ns NVT simulation at 600 K
4. 0.1 ns NPT simulation at 600 K and 1 bar

The above procedure was looped until convergence of the system density. In the equilibration part, the temperature and pressure are coupled by Berendsen thermostat and barostat,[S1] the corresponding coupling constants are 0.5 and 1.0 ps, respectively. The leap-frog verlet algorithm was used as an integrator. The time step was set to 1 fs, the cutoffs for the van der Waals and the long-range electrostatic interactions were set to 1.2 nm, the long-range electrostatic interactions were calculated with the particle mesh method (PME).[S2] All bonds that include hydrogen atoms were constrained using the LINCS algorithm.[S3]

The OPLS-like force field parameters were using for describing the intertactions,[S4] explictly, the parameters for the 1-n-butyl,3-methylimidazolium hexafluorophosphate ($[BvIm]^+$-$[PF_6]^-$) were obtained from Doherty and coworkers' work,[S5] the parameters for polymeric system (poly$[BvIm]^+[PF_6]^-$) can be found in our previous studies,[S6–S8] the full charges are used without any charge scaling parameter.

Table S1: System setup for varying the degree of polymerization N, the total number of ion pairs is about 1600.

System	N1	N2	N3	N4	N6	N8
$n_{polyILs}$	1600	800	534	400	267	200
n_{BmIm^+}	1600	1600	1602	1600	1602	1600
$n_{PF_6^-}$	1600	1600	1602	1600	1602	1600

For the production part, most of the parameters for the MD are the same to those used in the equilibration portion of the simulation. The integrator for the equation of motion is based on the velocity Verlet algorithm.[S9] The temperature is coupled by the Nosé-Hoover thermostat[S10] and the pressure is coupled by the Martyna-Tuckerman-Tobias-Klein (MTTK) barostat.[S11,S12] A total simulation time of 410 ns has been used for the production runs, except for the N1 (40 ns) and N6 (70 ns). The first 10 ns simulation for all the systems has been considered as an equilibration and the trajectories from this 10 ns simulation are not used for any analysis posed later.

S2.2 Non-equilibrium Simulations

For the non-equilibrium MD simulation,[S13–S15] the strength of the external electric field is varied between 0.001 to 0.010 V/Å with an increment of 0.001 V/Å. We used three samples for averaging the results: the external electric field has been applied to X direction for the first sample, Y direction for the second sample and Z direction for the third sample. A simulation of 40 ns has been used for each of the data point.

All simulations were performed by using GROMACS 2018.4,[S16] and all the post-processing were analyzed by the *in-house* code UTAnalysis, which is available upon the request to the authors.

S3 Diffusion Coefficient D and Ionic Mobility μ

S3.1 Linear Fitting for the Diffusion Coefficient D

The diffusion coefficient D is normally been calculated by using the Einstein equation from the respective mean-squared displacement (MSD),

$$D = \lim_{t\to\infty} \frac{1}{6t} \langle (r(t) - r(0))^2 \rangle \tag{S12}$$

where $r(t)$ denotes the center-of-mass position of anion or cation at time t. To account for the fact that cation diffusivities may not necessarily reach the linear regime, we used the following fit to the long time diffusivities:

$$\frac{\langle (r(t) - r(0))^2 \rangle}{6t} = D + A \cdot t^{-1} \tag{S13}$$

The D was then be fitted from equation S13 with a time window of 150 ns for anion (100 ns for cation). In our results, equation S12 has been used for fitting the D for N1 and N2, and the averaged results from equation S12 and S13 are used for N3 and later. The fits based on such an equation are displayed in the next two sections.

S3.1.1 Anion PF_6^- part I

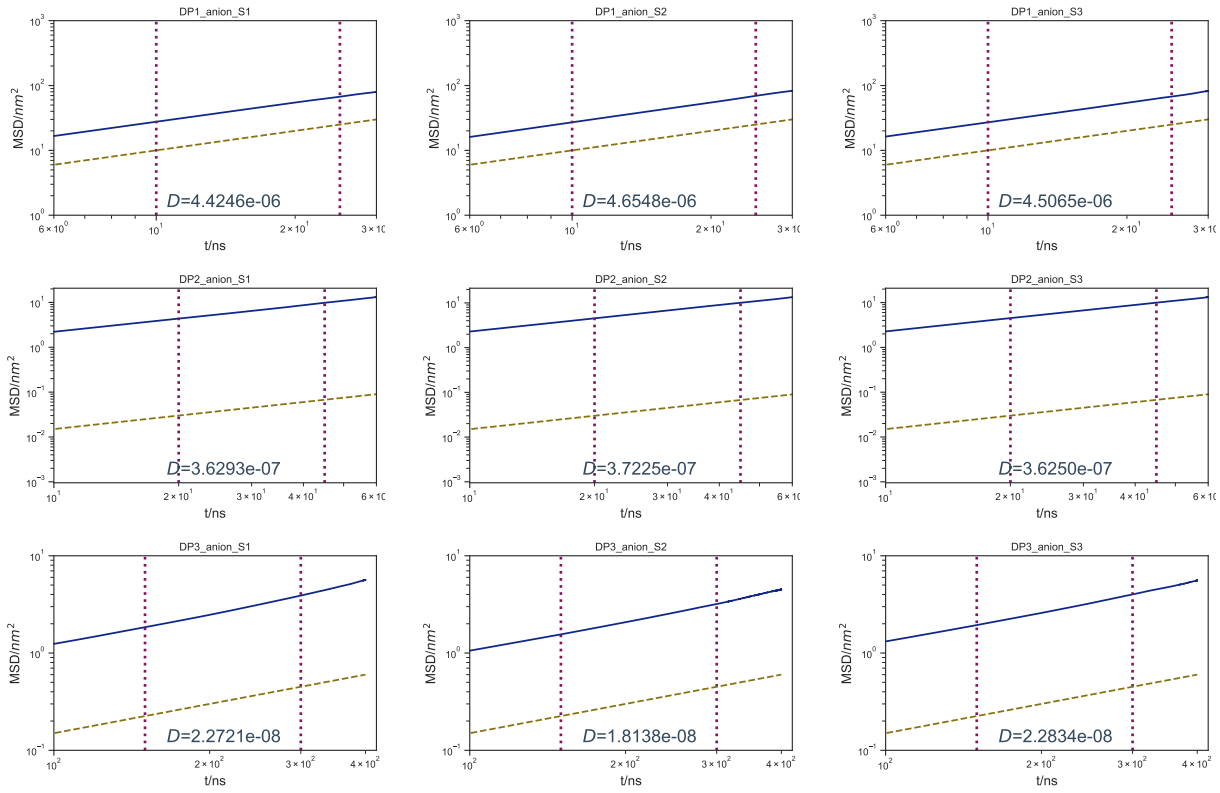

Figure S1: The log-log plot for anion MSDs, the yellow dash line has a slope of 1.0 and used as the benchmark for the fitting of diffusion coefficient D, range between two purple dotted lines are used for the fitting (top panel: N1, middle panel: N2 and bottom panel: N3, three columns indicate the results from three independent samples).

S3.1.2 Anion PF_6^- part II

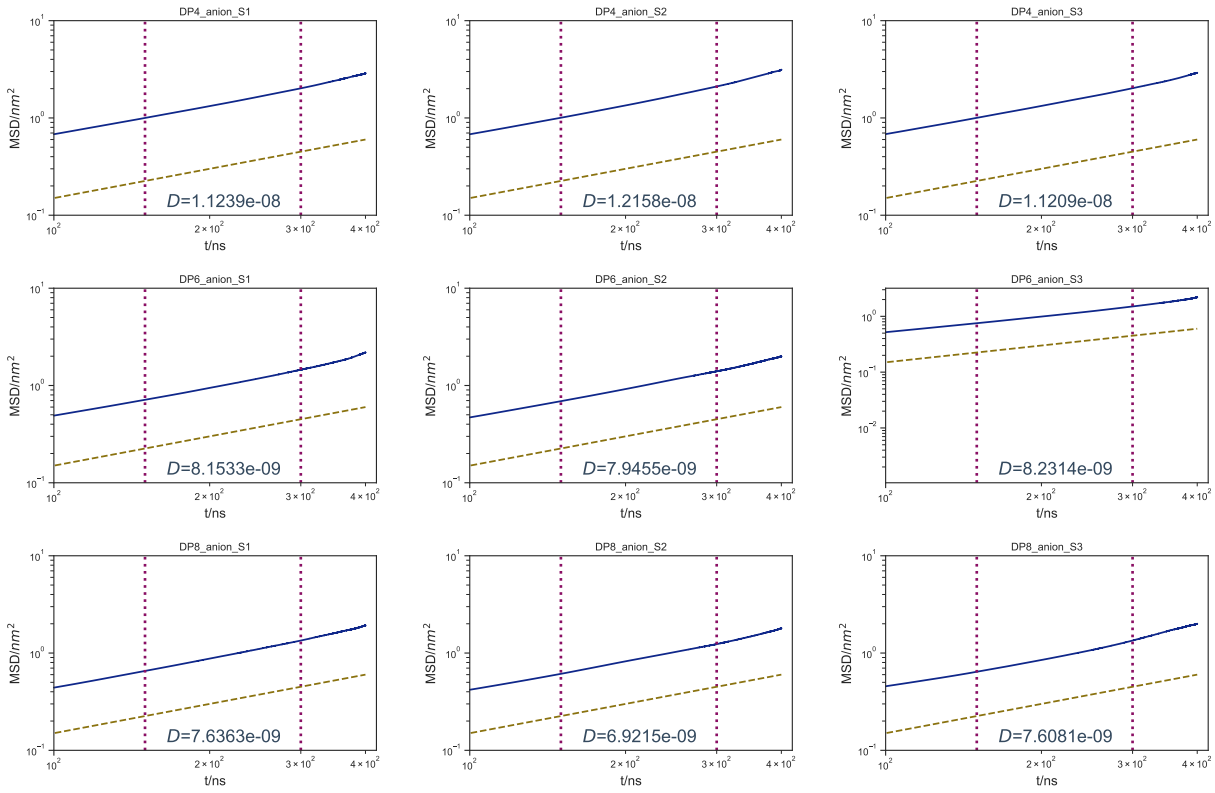

Figure S2: The log-log plot for anion MSDs, the yellow dash line has a slope of 1.0 and used as the benchmark for the fitting of diffusion coefficient D, range between two purple dotted lines are used for the fitting (top panel: N4, middle panel: N6 and bottom panel: N8, three columns indicate the results from three independent samples).

S3.1.3 Cation $BmIm^+$ part I

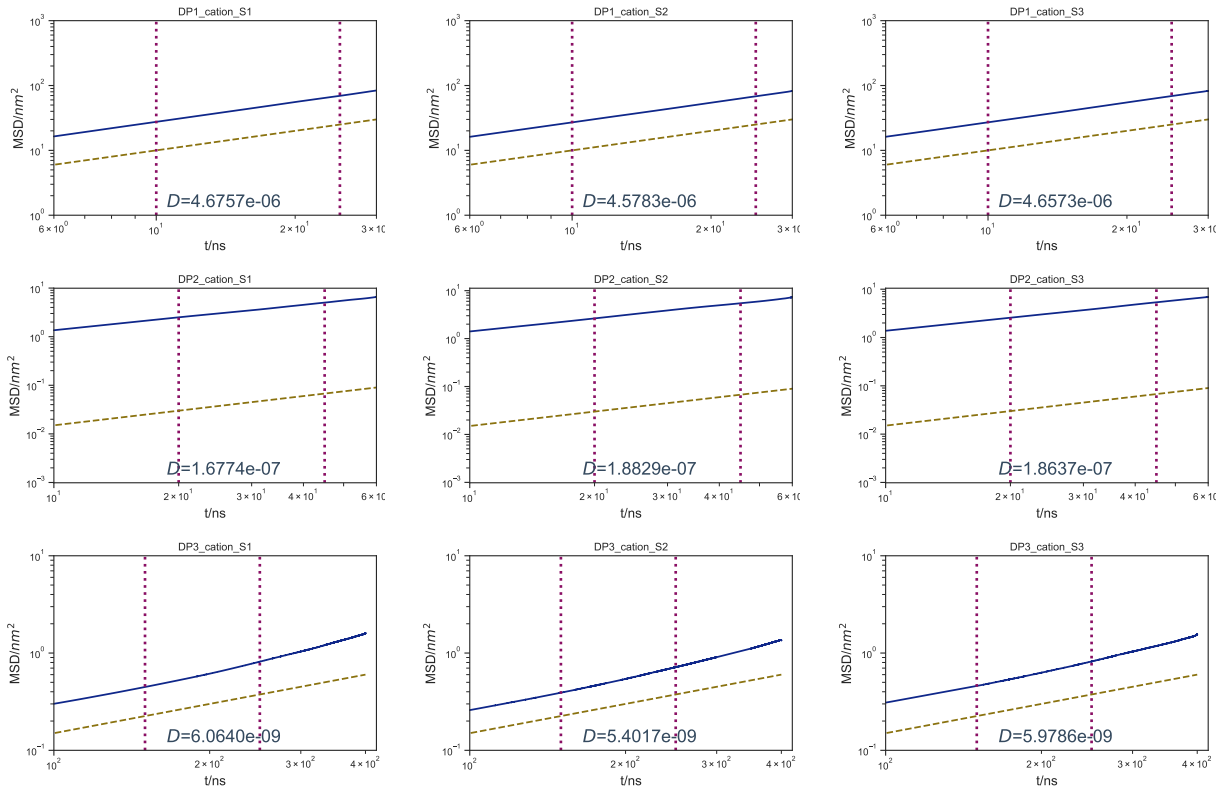

Figure S3: The log-log plot for cation MSDs, the yellow dash line has a slope of 1.0 and used as the benchmark for the fitting of diffusion coefficient D, range between two purple dotted lines are used for the fitting (top panel: N1, middle panel: N2 and bottom panel: N3, three columns indicate the results from three independent samples).

S3.1.4 Cation $BmIm^+$ part II

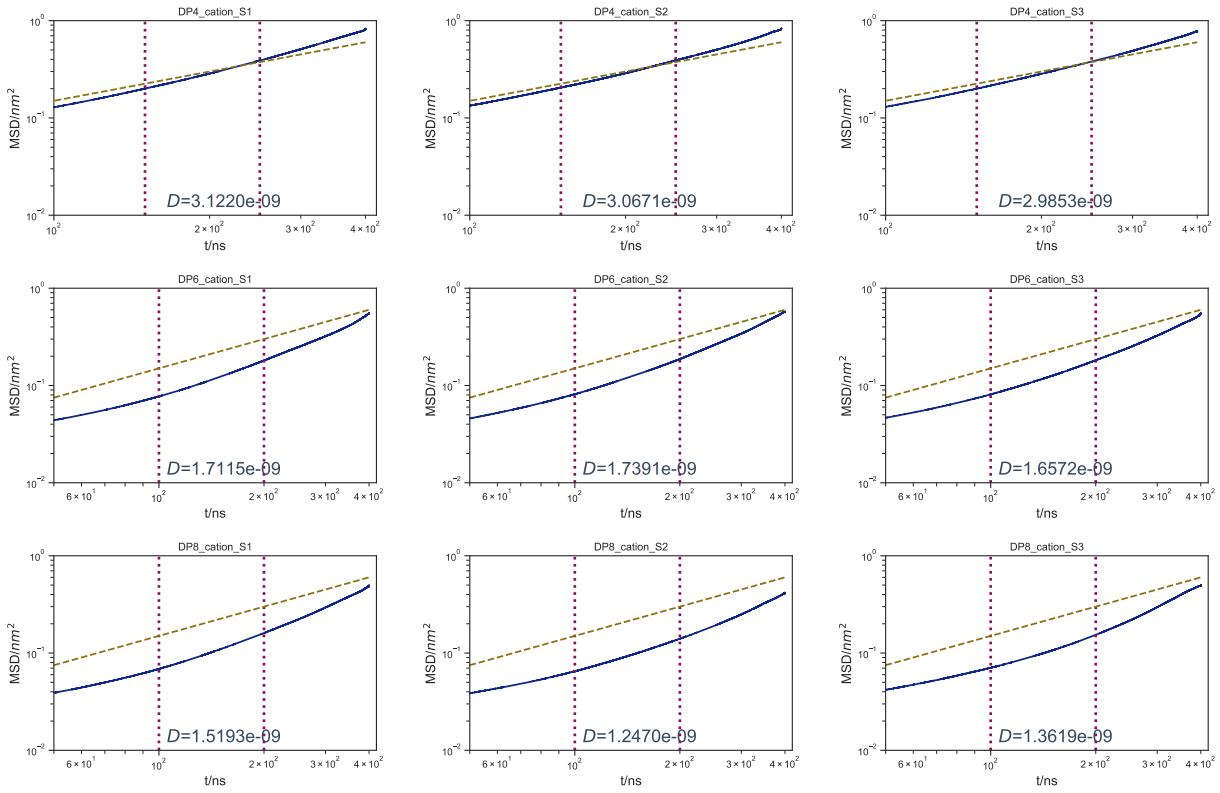

Figure S4: The log-log plot for cation MSDs, the yellow dash line has a slope of 1.0 and used as the benchmark for the fitting of diffusion coefficient D, range between two purple dotted lines are used for the fitting (top panel: N4, middle panel: N6 and bottom panel: N8, three columns indicate the results from three independent samples).

S3.2 Non-linear Fitting for the Diffusion Coefficient D

To provide an independent fit of the mean-squared displacements and diffusion coefficients, we also used the following equation:

$$\frac{\langle (r(t) - r(0))^2 \rangle}{6t} = D \cdot ((\frac{t}{\tau})^{-(1-\alpha)\gamma} + 1)^{1/\gamma}. \tag{S14}$$

The above function is proposed as a simple extrapolation between the short-time subdiffusive regimes of the mean-squared displacements (t^α, $\alpha < 1$) to its long-time linear regime. The parameter τ denotes a crossover time between the subdiffusive and long-time regimes. The fits based on such an equation are displayed in the next two subsections.

S3.2.1 Anion PF_6^-

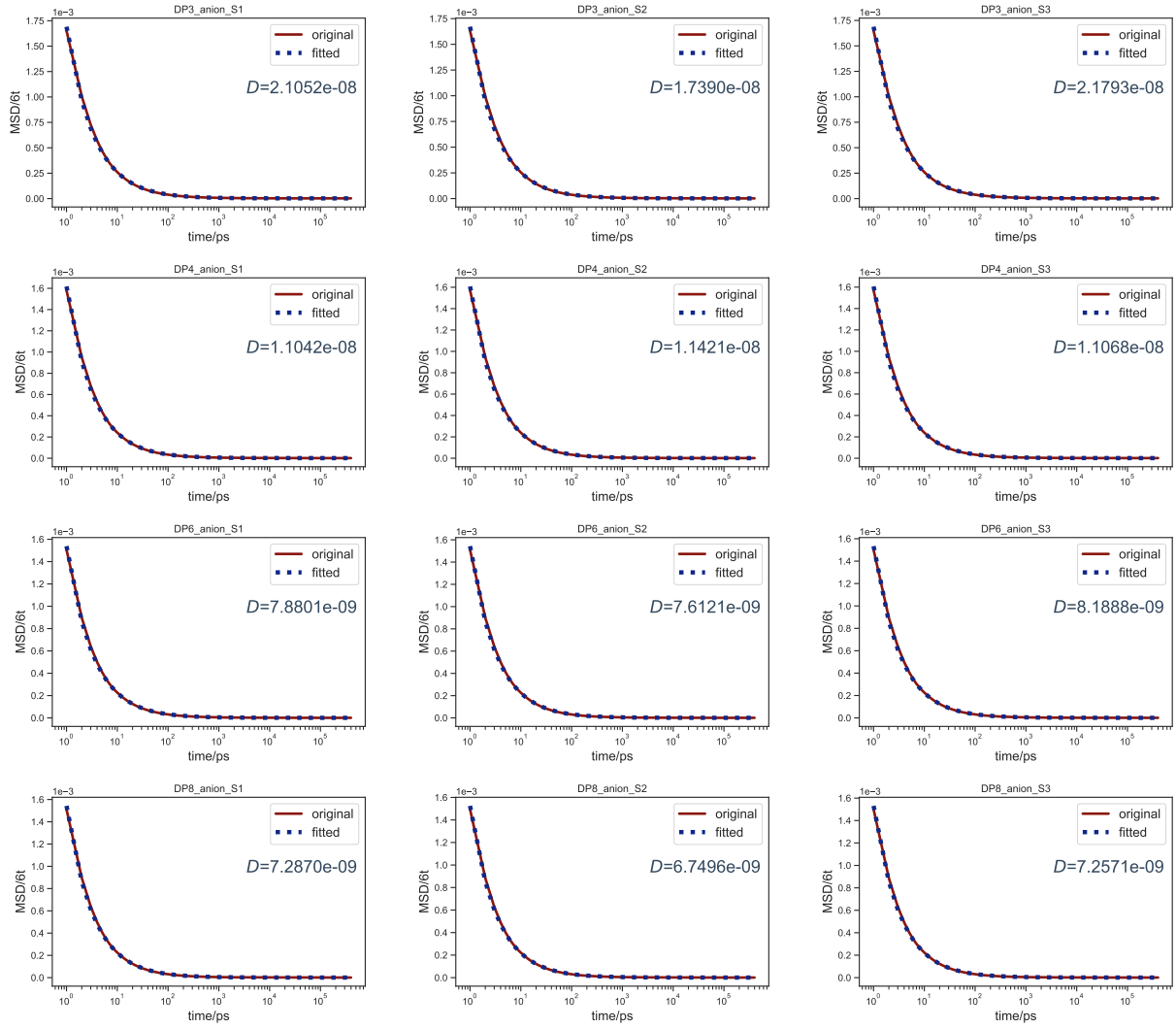

Figure S5: The non-linear fitting of anionic diffusion coefficient D by using equation S14 (top panel: N3, second panel: N4, third panel: N6 and bottom panel: N8, three columns indicate the results from three independent samples).

S3.2.2 Cation $BmIm^+$

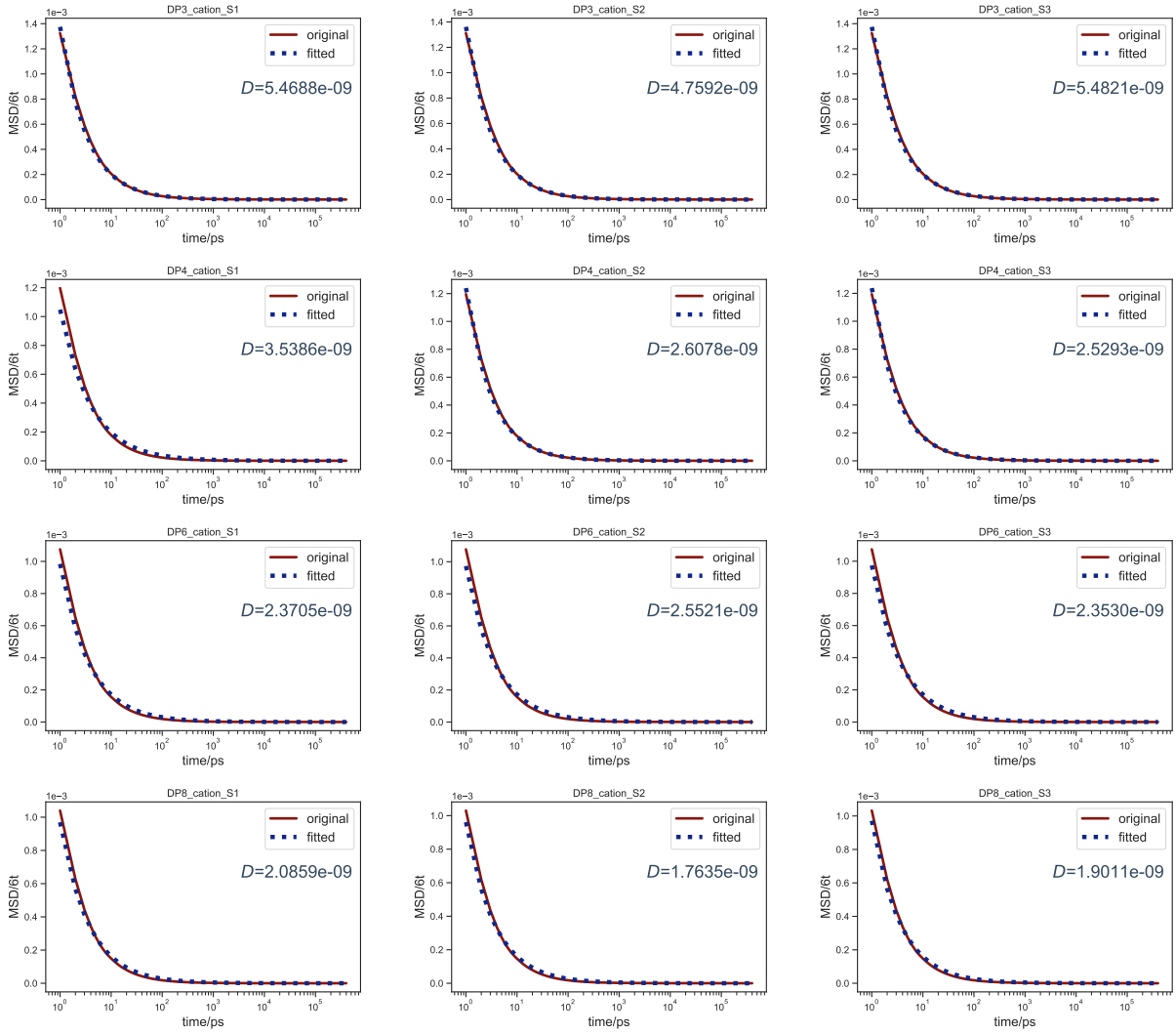

Figure S6: The non-linear fitting of cationic diffusion coefficient D by using equation S14 (top panel: N3, second panel: N4, third panel: N6 and bottom panel: N8, three columns indicate the results from three independent samples).

S3.3 Linear Response Regime for Fitting Ionic Mobility μ

The ionic mobility (μ) is extracted from the linear response regime, as mentioned in the **Simulation Details** section. Ten external electric fields have been used for fitting the mobilities in the linear response regime. From the results shown below we can see that for most of the cases the last two points do not fall under the linear response regime, and hence only the first eight points are used for fitting μ,

$$\mu = \frac{\langle v \rangle_i}{E} \tag{S15}$$

where $\langle v \rangle_i$ ($i \in [X, Y, Z]$, X, Y, Z are the directions that the electric field applied) is the drift velocity and E is the strength of the external electric field.

The drift velocity $\langle v \rangle_i$ is calculated from the linear regression of the displacement Δr_i versus time t.

$$\Delta r_i = \lim_{t \to \infty} \langle r_i(t + t_0) - r_i(t_0) \rangle \tag{S16}$$

To reduce the statistical uncertainty in the calculation of Δr_i, each configuration is treated as a time reference (t_0).

S3.3.1 Results and fit of nonequilibrium simulations

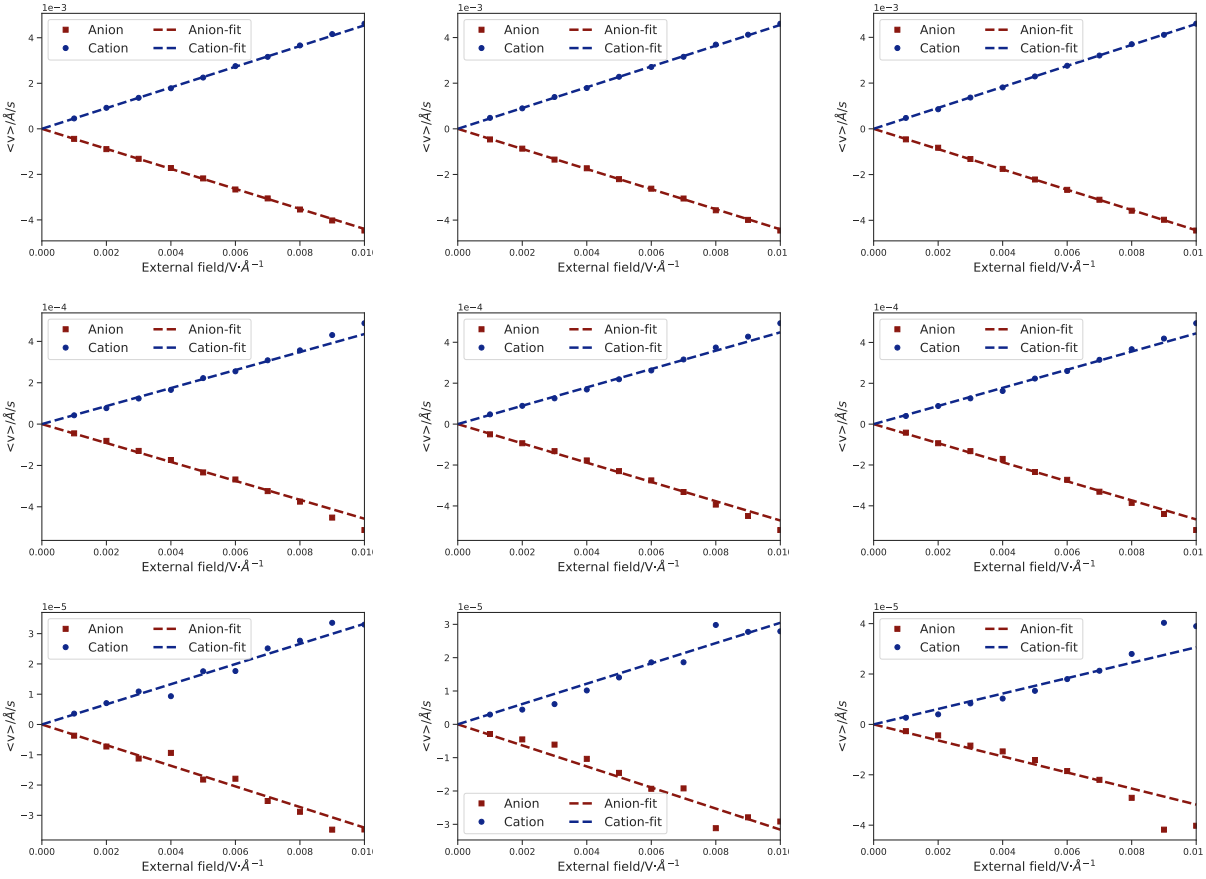

Figure S7: Effect of external electric fields on drift velocity $\langle v \rangle$ (top panel: N1, middle panel: N2 and bottom panel: N3, three columns indicate the results from three independent samples).

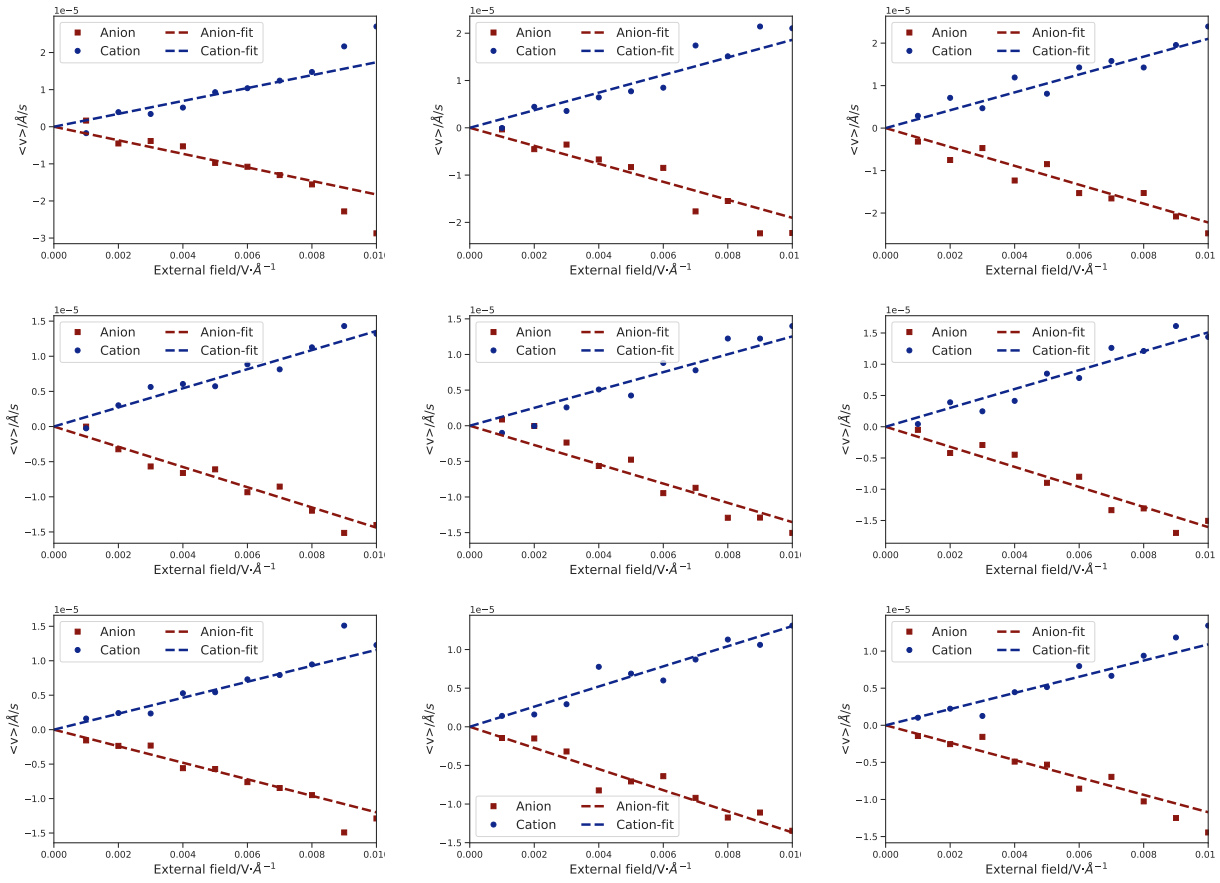

Figure S8: Effect of external electric fields on drift velocity $\langle v \rangle$ (top panel: N4, middle panel: N6 and bottom panel: N8, three columns indicate the results from three independent samples).

S4 Ratios of conductivity components to the "true" conductivity σ

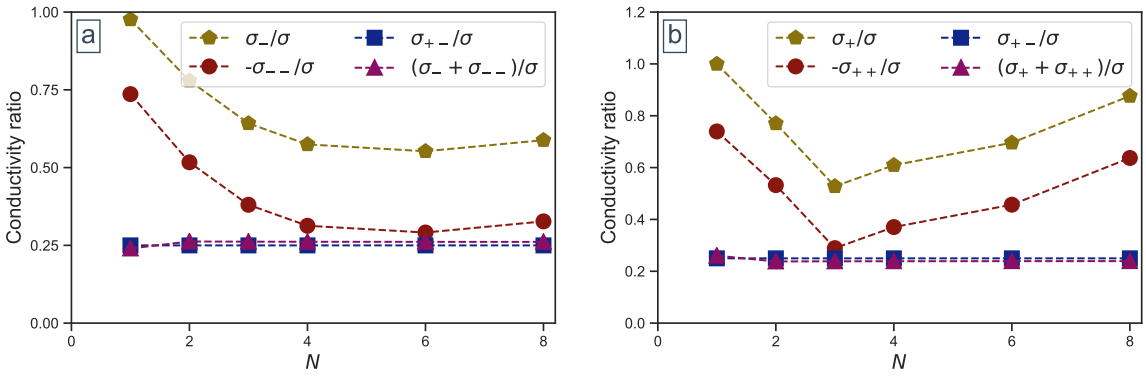

Figure S9: Ratios of the absolute individual conductivity to the *true* conductivity σ, (a) anion related conductivity terms, and (b) cation related conductivity terms.

S5 Influence of choice of reference frame on the contributions of different ion correlations to the overall conductivity

In this section, we discuss the influence of the choice of reference frame on the values of the distinct diffusion coefficients. To recall, in this specific work, we chose the reference frame as the center of mass of the system. However, other choices of the reference frame exist. In particular, the polymer itself may be a useful reference frame especially in the case of very high molecular weights. However, as we discuss below, the choice of the reference frame does not influence the self-diffusivities or the overall conductivity. Instead, the reference frame can only influence the contributions ascribed to the distinct diffusivities and conductivities. We draw the essentials of our derivation from Appendix D of Kashyap and coworkers' work.[S17]

According to Kashyap and coworkers, the distinct polymer diffusion coefficient can be expressed as

$$D_p^d = \frac{1}{3N_p^2}\int_0^\infty \sum_{i_p}^{N_p}\sum_{j_p\neq i_p}^{N_p} \left\langle N\left[\mathbf{v}_{i_p}(t)-\mathbf{w}_R(t)\right]\cdot\left[\mathbf{v}_{j_p}(0)-\mathbf{w}_R(0)\right]\right\rangle \mathrm{d}t \tag{S17}$$

where N, N_p, and $v_{i_p}(t)$ are the total number of ions in the system, number of cationic polymers in the system, and the velocity of polymer i_p at time t. We can define a velocity $\mathbf{v}_p(t)$ is the average polymer velocity (a similar velocity can be defined for counteranions a) in the laboratory reference frame

$$\mathbf{v}_p(t) = \frac{1}{N_p}\sum_{i_p}^{N_p}\mathbf{v}_{i_p}(t) \tag{S18}$$

Using the average velocities derived by using Equation S18, we can define the reference frame

velocity $w_R(t)$, which is the weighted average of the average and counteranion velocities

$$\mathbf{w}_R(t) = a_p^R \mathbf{v}_p(t) + a_a^R \mathbf{v}_a(t) \tag{S19}$$

where $a_p^R + a_a^R = 1$ and $a_i \in [0, 1]$. Substituting the average velocity definition in Equation S18 into Equation S17, we can express D_p^d as a function of average velocities and self terms

$$\begin{aligned} D_p^d = \frac{N}{3} \int_0^\infty \Bigg\{ & \langle [\mathbf{v}_p(t) - \mathbf{w}_R(t)] \cdot [\mathbf{v}_p(0) - \mathbf{w}_R(0)] \rangle \\ & - \frac{1}{N_p^2} \sum_{i_p}^{N_p} \left\langle \left[\mathbf{v}_{i_p}(t) - \mathbf{w}_R(t)\right] \cdot \left[\mathbf{v}_{i_p}(0) - \mathbf{w}_R(0)\right] \right\rangle \Bigg\} \, \mathrm{d}t \end{aligned} \tag{S20}$$

We define a differential velocity

$$\mathbf{v}^e(t) = \mathbf{v}_p(t) - \mathbf{v}_a(t) \tag{S21}$$

Combining Equations S19 and S21, we can show that

$$\begin{aligned} \mathbf{v}_p(t) - \mathbf{w}_R(t) &= \mathbf{v}_p(t) - a_p^R \mathbf{v}_p(t) - a_a^R \mathbf{v}_a(t) \\ &= (1 - a_p^R) \mathbf{v}^e(t) \end{aligned} \tag{S22}$$

Additionally, we recognize that the second term in Equation S20 is related to the self-diffusion coefficient

$$D_p^s = \frac{1}{3N_p} \int_0^\infty \left\langle \left[\mathbf{v}_{i_p}(t) - \mathbf{w}_R(t)\right] \cdot \left[\mathbf{v}_{i_p}(0) - \mathbf{w}_R(0)\right] \right\rangle \mathrm{d}t \tag{S23}$$

We observe (by expanding the above equation) that the self-diffusion coefficient is independent of the reference frame.[S18] Combining Equations S20, S22, and S23, the reference frame

velocity $\mathbf{w}_R(t)$ drops out, and D_p^d gains dependence on the self-diffusion coefficient D_p^s

$$D_p^d = -\frac{D_p^s}{x_p} + \frac{N(1-a_p^R)^2}{3}\int_0^\infty \langle \mathbf{v}^e(t)\cdot\mathbf{v}^e(0)\rangle \,\mathrm{d}t \tag{S24}$$

where x_p is the polymer molar fraction. Kashyap showed that the conductivity σ is related to the rightmost integral (and is also thus independent of reference frame):[S17]

$$\sigma\left(\frac{3k_BT}{\rho e^2(z_p x_p)^2}\right) = N\int_0^\infty \langle \mathbf{v}^e(t)\cdot\mathbf{v}^e(0)\rangle \,\mathrm{d}t \tag{S25}$$

where k_B is the Boltzmann constant, T is the temperature, ρ is the density, e is the proton charge, z_p is the polymer charge, and x_p is the volume fraction of polymer. Thus, combining S24 and S25 yields

$$D_p^d = -\frac{D_p^s}{x_p} + \left(\frac{k_BT(1-a_p^R)^2}{\rho e^2(z_p x_p)^2}\right)\sigma \tag{S26}$$

Kashyap similarly derived an expression for the distinct polymer-anion diffusion coefficient D_{pa}^d:[S17]

$$D_{pa}^d = -\left(\frac{k_BT(1-a_p^R)a_p^R}{\rho e^2(z_p x_p)^2}\right)\sigma \tag{S27}$$

A similar derivation can be done for the anion distinct coefficient D_a^d, yielding

$$D_a^d = -\frac{D_a^s}{1-x_p} + \left(\frac{k_BT(a_p^R)^2}{\rho e^2(z_p x_p)^2}\right)\sigma \tag{S28}$$

It is clear from Equations S26–S28 that correlations assigned to each distinct coefficient vary when the reference frame is changed (by varying a_p). **In the case of the polymer-centered reference frame ($a_p = 1$), $D_{pa}^d = 0$, $D_p^d = -D_p^s/x_p$, and all cross-correlations are captured by D_a^d.**

The result for diffusivity components and conductivity components are shown in the following figure by using the center of mass (COM) of the polymer chains as the reference

frame (figures that use the COM of entire system as the reference frame can be found in Fig.3 in main text). Nevertheless, the core results in the current paper, namely the inverse Haven ratio H^{-1} and *ideal* transference number (cf. eq. 3, main text) are independent from the choice of reference frame (while the individual conductivities σ_+ and σ_- do have correlations to the choice of reference frame), since the true conductivity and the self-diffusion coefficients are independent from the choice of reference frame.[S18]

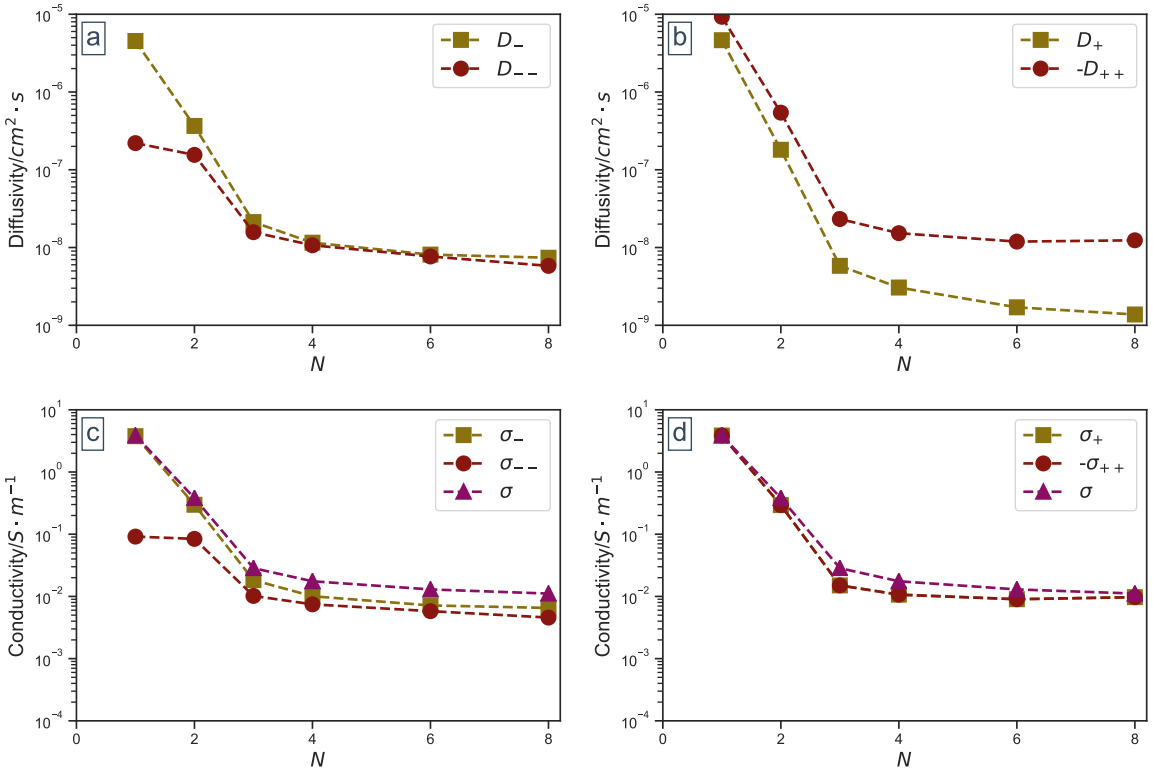

Figure S10: Self and distinct diffusion coefficients for anion (a) and cation (b) as a function of N, the anion related (c) and cation related (d) conductivity components as a function of N (the center of mass of the polymer chains is the reference frame).

References

(S1) Berendsen, H. J. C.; Postma, J. P. M.; van Gunsteren, W. F.; DiNola, A.; Haak, J. R. Molecular dynamics with coupling to an external bath. *The Journal of Chemical Physics* **1984**, *81*, 3684–3690.

(S2) Darden, T.; York, D.; Pedersen, L. Particle mesh Ewald: An N·log(N) method for Ewald sums in large systems. *The Journal of Chemical Physics* **1993**, *98*, 10089–10092.

(S3) Hess, B.; Bekker, H.; Berendsen, H. J. C.; Fraaije, J. G. E. M. LINCS: A linear constraint solver for molecular simulations. *Journal of Computational Chemistry* **1997**, *18*, 1463–1472.

(S4) Caleman, C.; van Maaren, P. J.; Hong, M.; Hub, J. S.; Costa, L. T.; van der Spoel, D. Force Field Benchmark of Organic Liquids: Density, Enthalpy of Vaporization, Heat Capacities, Surface Tension, Isothermal Compressibility, Volumetric Expansion Coefficient, and Dielectric Constant. *Journal of Chemical Theory and Computation* **2012**, *8*, 61–74.

(S5) Doherty, B.; Zhong, X.; Gathiaka, S.; Li, B.; Acevedo, O. Revisiting OPLS Force Field Parameters for Ionic Liquid Simulations. *Journal of Chemical Theory and Computation* **2017**, *13*, 6131–6145.

(S6) Mogurampelly, S.; Keith, J. R.; Ganesan, V. Mechanisms Underlying Ion Transport in Polymerized Ionic Liquids. *Journal of the American Chemical Society* **2017**, *139*, 9511–9514.

(S7) Keith, J. R.; Mogurampelly, S.; Aldukhi, F.; Wheatle, B. K.; Ganesan, V. Influence

of molecular weight on ion-transport properties of polymeric ionic liquids. *Physical Chemistry Chemical Physics* **2017**, *19*, 29134–29145.

(S8) Zhang, Z.; Krajniak, J.; Keith, J. R.; Ganesan, V. Mechanisms of Ion Transport in Block Copolymeric Polymerized Ionic Liquids. *ACS Macro Letters* **2019**, 1096–1101.

(S9) Swope, W. C.; Andersen, H. C.; Berens, P. H.; Wilson, K. R. A computer simulation method for the calculation of equilibrium constants for the formation of physical clusters of molecules: Application to small water clusters. *The Journal of Chemical Physics* **1982**, *76*, 637–649.

(S10) Evans, D. J.; Holian, B. L. The Nose–Hoover thermostat. *The Journal of Chemical Physics* **1985**, *83*, 4069–4074.

(S11) Martyna, G. J.; Tuckerman, M. E.; Tobias, D. J.; Klein, M. L. Explicit reversible integrators for extended systems dynamics. *Molecular Physics* **1996**, *87*, 1117–1157.

(S12) Tuckerman, M. E.; Alejandre, J.; López-Rendón, R.; Jochim, A. L.; Martyna, G. J. A Liouville-operator derived measure-preserving integrator for molecular dynamics simulations in the isothermal–isobaric ensemble. *Journal of Physics A: Mathematical and General* **2006**, *39*, 5629–5651.

(S13) Lee, S. H.; Rasaiah, J. C. Molecular dynamics simulation of ionic mobility. I. Alkali metal cations in water at 25 °C. *The Journal of Chemical Physics* **1994**, *101*, 6964–6974.

(S14) Ting, C. L.; Stevens, M. J.; Frischknecht, A. L. Structure and Dynamics of Coarse-Grained Ionomer Melts in an External Electric Field. *Macromolecules* **2015**, *48*, 809–818.

(S15) Alshammasi, M. S.; Escobedo, F. A. Correlation between Ionic Mobility and Microstructure in Block Copolymers. A Coarse-Grained Modeling Study. *Macromolecules* **2018**, *51*, 9213–9221.

(S16) Pronk, S.; Páll, S.; Schulz, R.; Larsson, P.; Bjelkmar, P.; Apostolov, R.; Shirts, M. R.; Smith, J. C.; Kasson, P. M.; van der Spoel, D.; Hess, B.; Lindahl, E. GROMACS 4.5: a high-throughput and highly parallel open source molecular simulation toolkit. *Bioinformatics* **2013**, *29*, 845–854.

(S17) Kashyap, H. K.; Annapureddy, H. V. R.; Raineri, F. O.; Margulis, C. J. How Is Charge Transport Different in Ionic Liquids and Electrolyte Solutions? *The Journal of Physical Chemistry B* **2011**, *115*, 13212–13221.

(S18) Raineri, F. O.; Friedman, H. L. The role of reference frames in the molecular theory of diffusive transport in solutions. *The Journal of Chemical Physics* **1989**, *91*, 5633–5641.